Crosstalk of the mTOR network with stress granules and the TGF-beta pathway

Prentzell, Mirja Tamara

CHAPTER 5

PI3K-p110-alpha-subtype signalling mediates survival, proliferation and neurogenesis of cortical progenitor cells via activation of mTORC2

Shalaka Dhanraj Wahane [*,†,1], Nicole Hellbach [*,†,1], **Mirja Tamara Prentzell** [‡,§,1], Stefan Christopher Weise [*,†], Riccardo Vezzali [*,†], Clemens Kreutz [¶,**], Jens Timmer [¶,**,††], Kerstin Krieglstein [*,††], Kathrin Thedieck [**,††,‡‡,§§,2], Tanja Vogel [*,2]

[*]Department of Molecular Embryology, Institute of Anatomy and Cell Biology, Albert-Ludwigs-University Freiburg, Freiburg, Germany
[†]Faculty of Biology, Albert-Ludwigs-University Freiburg, Freiburg, Germany
[‡]Department of Bioinformatics and Molecular Genetics, Faculty of Biology, Albert-Ludwigs-University Freiburg, Freiburg, Germany
[§]Spemann Graduate School of Biology and Medicine (SGBM), Albert-Ludwigs-University Freiburg, Freiburg, Germany
[¶]Institute of Physics, Albert-Ludwigs-University Freiburg, Freiburg, Germany
[**]Center for Systems Biology (ZBSA), Albert-Ludwigs-University Freiburg, Freiburg, Germany
[††]BIOSS Centre for Biological Signalling Studies, Albert-Ludwigs-University Freiburg, Freiburg, Germany
[‡‡]Center for Liver, Digestive and Metabolic Diseases, Department of Pediatrics, University of Groningen, University Medical Center Groningen, Groningen, The Netherlands
[§§]School of Medicine and Health Sciences, Carl von Ossietzky University Oldenburg, Oldenburg, Germany
[1]These authors contributed equally as first authors.
[2]These authors contributed equally as senior authors.

Journal of Neurochemistry, 2014
PMID: 24645666

ABSTRACT

Development of the cerebral cortex is controlled by growth factors among which transforming growth factor beta (TGFβ) and insulin-like growth factor 1 (IGF1) have a central role. The TGFβ- and IGF1-pathways cross-talk and share signalling molecules, but in the central nervous system putative points of intersection remain unknown. We studied the biological effects and down-stream molecules of TGFβ and IGF1 in cells derived from the mouse cerebral cortex at two developmental time points, E13.5 and E16.5. IGF1 induces PI3K, AKT and the mammalian target of rapamycin complexes (mTORC1/mTORC2) primarily in E13.5-derived cells, resulting in proliferation, survival and neuronal differentiation, but has small impact on E16.5-derived cells. TGFβ has little effect at E13.5. It does not activate the PI3K- and mTOR-signalling network directly, but requires its activity to mediate neuronal differentiation specifically at E16.5. Our data indicate a central role of mTORC2 in survival, proliferation as well as neuronal differentiation of E16.5-derived cortical cells. mTORC2 promotes these cellular processes and is under control of PI3K-p110-alpha signalling. PI3K-p110-beta signalling activates mTORC2 in E16.5-derived cells but it does not influence cell survival, proliferation and differentiation. This finding indicates that different mTORC2 subtypes may be implicated in cortical development and that these subtypes are under control of different PI3K isoforms.

Keywords

brain, cerebral cortex, insulin, neuron, PI3K-isoform, PI3K-subunit.

INTRODUCTION

Development of the cerebral cortex is a tightly orchestrated process that requires specific activities of cell intrinsic and extrinsic cues. Amongst the latter is a plethora of cytokines and signalling molecules. Proliferation, survival, and differentiation in the cerebral cortex are under the control of several signalling pathways, including transforming growth factor beta (TGFβ) and insulin/insulin-like growth factor (IGF) (Ye and D'Ercole 2006). In the cerebral cortex TGFβ promotes neuronal differentiation in a SMAD-dependent manner (Vogel *et al*. 2010) and is implicated in generation of Cajal-Retzius cells in the cortical hem (Siegenthaler and Miller 2008). Insulin/IGF-signalling (IIS) has multiple effects during development of the cerebral cortex, including neuronal differentiation (Arsenijevic and Weiss 1998; Han *et al*. 2008a) and proliferation of cortical progenitors (Ajo *et al*. 2003; Mairet-Coello *et al*. 2009). IIS has pleiotropic effects at different developmental stages, for example adult hippocampal neurons respond to IGF1 by proliferating (Aberg *et al*. 2003), whereas in contrast embryonic hippocampal progenitors require IIS for their survival (Zheng *et al*. 2002). In cells other than neurons the signalling cascades of both TGFβ and IIS pathways have been studied in great detail. Several points of intersection and potential cross-talk have been identified (Danielpour and Song 2006), however, these investigations were not conducted in cells from the central nervous system (CNS). In other cellular systems, class I-phosphoinositide 3-kinases (PI3K) and Protein kinase B (AKT, also named PKB) stand out among proteins that are under the control of both insulin/IGF and TGFβ. Studies of TGFβ-signalling utilizing PI3K-AKT in the CNS are rare. Consequently, cross-talk of TGFβ- and IGF-signalling pathways in the CNS at the level of PI3K-AKT has so far not been studied.

A further point of intersection in non-neuronal cells is the mammalian target of rapamycin (mTOR) kinase that initiates an important down-stream pathway under the control of IIS, but also of TGFβ (Song *et al*. 2006). mTOR is a central regulator of cellular growth, survival and differentiation (Laplante and Sabatini 2012). mTOR exists in two structurally and functionally distinct multiprotein complexes, mTORC1 and mTORC2. mTORC1 is acutely inhibited by the allosteric inhibitor Rapamycin, and thus Rapamycin effects can be largely assigned to mTORC1. It should be noted though that also rapamycin-insensitive effects of mTORC1 on autophagy and translation have been reported (Thoreen and Sabatini 2009; Thoreen *et al*. 2009; Kang *et al*. 2013). mTORC2 is Rapamycin insensitive in most tested cell types (Sarbassov *et al*. 2006); in few cell types with low mTOR levels prolonged Rapamycin exposure can indirectly inhibit mTORC2 (Sarbassov *et al*. 2006; Lamming *et al*. 2012; Urbanska *et al*. 2012).

mTORC1 responds to IIS via the insulin/IGF receptors (IR, IGFR), which upon activation and autophosphorylation at tyrosines 980 and 1135 activate PI3Ks via the Insulin Receptor Substrate-1 (IRS-1). Active PI3K recruits AKT to the plasma membrane where it can be activated by phosphoinositide-dependent protein kinase 1 (PDK1) through phosphorylation in the activation loop (AKT-pT308). Activated AKT stimulates mTORC1 activity. Although mTORC2 also responds to IIS, the mechanism is comparatively poorly understood. This is in part because of the fact that no mTORC2-specific inhibitors are available so far. It has recently been discovered that mTORC2 function depends on PI3K, yet this PI3K input is independent of AKT, and therefore different to the PI3K input of mTORC1 (Dalle Pezze *et al*. 2012; Sonntag *et al*. 2012).

Rapamycin blocks mitosis but not survival of cortical progenitors (Sinor and Lillien 2004). In neurospheres from neonatal rat telencephalon, Rapamycin blocks neuronal differentiation (Han *et al*. 2008b). Rapamycin-treatment of adult hippocampus-derived progenitors interferes with proliferation (Peltier *et al*. 2007), but has little effect on proliferation in another study (Aberg *et al*. 2003). These studies suggest that mTORC1 has a role during cerebral development. However, a possible function of mTORC2 is entirely elusive. Inhibitors for both mTOR complexes, like Torin1 (Thoreen *et al*. 2009), have become available only recently and therefore give new opportunity to study the contribution of each complex in greater detail.

In this study we determined the developmental dynamics of TGFβ-, IGF- and mTOR-signalling and their putative cross-talk in E13.5- as compared to E16.5-derived cortical cells in culture. E13.5 cortical cells mainly undergo proliferation, whereas neuronal differentiation predominates at E16.5 (Takahashi *et al*. 1996). We report the differential expression of TGFβ- and IIS-pathway components in cultured cortical cells derived from both developmental time points and a PI3K-p110-alpha-dependent mTORC2 activation that mediates proliferation, survival and neuronal differentiation of E16.5-derived cortical cells. TGFβ does not directly activate the AKT-mTOR pathway, but needs active PI3K-mTOR-signalling to mediate neuronal differentiation of cortical cells.

EXPERIMENTAL PROCEDURES

The detailed experimental description and used materials are outlined in the supplement.

Primary culture of cortical cells

As previously described (Vogel *et al*. 2010), cortical cells from embryonic stages E13.5 and E16.5 were dissected, cultured and treated with TGFβ (5 ng/mL), IGF1, IGF2 (both 10 nM) and/or following inhibitors SB431542 (10 μM), Picropodophyllin (PPP) (500 nM), MK-2206 (1 μM), A66 (10 μM), TGX-221 (2 μM), Rapamycin (100 nM) and Torin1 (250 nM) as well as dimethylsulfoxide (DMSO) (1 : 1000) for the durations indicated in Fig. 1a.

Immunocytochemistry (ICC)

Cells were either fixed on DIV6 or DIV8 according to experimental setup (Fig. 1a). Bromodeoxyuridine (BrdU) was applied at DIV6 for 1 h. Cells were permeabilized with acetone, blocked with 10% serum, 0.1% Triton X-100 and phosphate-buffered saline and incubated overnight at 4°C with the primary antibody. Used antibodies and dilutions are described in the supplement. At least eight images were quantified using a self-made macro for ImageJ (NIH, Bethesda, MD, USA).

Microarray analyses

Gene expression of E13.5- and E16.5-derived cortical cells treated with TGFβ or SB431542 were analysed using Agilent′s Mouse Genome Microarray (G4846A).

Real-time cell analyses

Real-time cell analyses (RTCA)-system (xCELLigence, Roche, Basel, Switzerland) was used to monitor proliferation, survival and cell death for 72 h. Inhibitors were added to the cells after 24 h (E13.5) or 8 h (E16.5) (Fig. 1a). For data analyses, each curve was normalized to the point of treatment (indicated in Figs 2d, 3a, b, h by the dashed vertical line). One representative experiment is shown.

Immunoblotting

Cells were lysed in RIPA buffer (1% NP-40, phosphate-buffered saline, 1% sodium dodecyl sulfate, and 0.5% sodium dodecyl sulfate), supplemented with protease- (Roche) and phosphatase-inhibitors (Phosphatase Inhibitor Cocktail 3, Sigma, St Louis, MO, USA) and sonicated in a Bioruptor (Diagenode) for 10 cycles with 10 s intervals. Protein concentration was measured with Bradford assay (Bio-Rad Laboratories, Hercules, CA, USA), adjusted with 5x Lämmli buffer. Denatured samples were run on 8–15% sodium dodecyl sulfate poly-acrylamide gels at 100 V for 1.5 h, transferred onto Polyvinylidene difluoride membranes (Merck Millipore, Billerica, MA, USA) for 1.5 h. Membranes were blocked for 20 min in 5% bovine serum albumin (Roth, Karlsruhe, Germany) solution in 1x

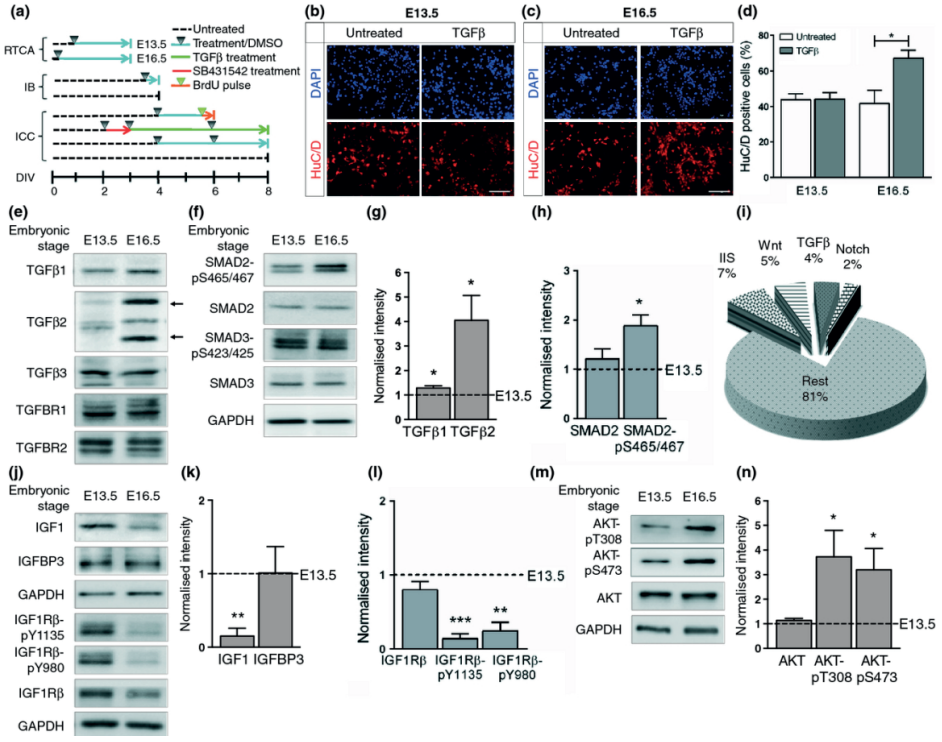
(a)
RTCA
IB
ICC
DIV
E13.5
E16.5
Untreated
Treatment/DMSO
TGFβ treatment
SB431542 treatment
BrdU pulse
0
2
4
6
8
(b)
E13.5
Untreated
TGFβ
DAPI
HuC/D
(c)
E16.5
Untreated
TGFβ
DAPI
HuC/D
(d)
Untreated
TGFβ
HuC/D positive cells (%)
E13.5
E16.5
(e)
Embryonic stage
E13.5
E16.5
TGFβ1
TGFβ2
TGFβ3
TGFBR1
TGFBR2
(f)
Embryonic stage
E13.5
E16.5
SMAD2-pS465/467
SMAD2
SMAD3-pS423/425
SMAD3
GAPDH
(g)
Normalised intensity
E13.5
TGFβ1
TGFβ2
(h)
Normalised intensity
E13.5
SMAD2
SMAD2-pS465/467
(i)
IIS 7%
Wnt 5%
TGFβ 4%
Notch 2%
Rest 81%
(j)
Embryonic stage
E13.5
E16.5
IGF1
IGFBP3
GAPDH
IGF1Rβ-pY1135
IGF1Rβ-pY980
IGF1Rβ
GAPDH
(k)
Normalised intensity
E13.5
IGF1
IGFBP3
(l)
Normalised intensity
E13.5
IGF1Rβ
IGF1Rβ-pY1135
IGF1Rβ-pY980
(m)
Embryonic stage
E13.5
E16.5
AKT-pT308
AKT-pS473
AKT
GAPDH
(n)
Normalised intensity
E13.5
AKT
AKT-pT308
AKT-pS473

Figure 1. Transforming growth factor beta (TGFβ)- and insulin-like growth factor (IGF)-signalling activities were different in E13.5- and E16.5-derived cortical cells.
(a) Treatment schemes for real-time cell analyses (RTCA), immunoblots (IB) and immunocytochemistry (ICC). Black triangle: time point of treatment. Dotted line: untreated cells. Solid lines: treatment duration; blue: duration of treatments with growth factors and/or inhibitors, red: SB431542-treatment at DIV2, green: TGFβ-treatment starting at DIV3. Short-term treatments with growth factors and inhibitors in immunoblots are denoted at DIV4 by black triangle and blue line. Green triangle and orange line: time point and duration of BrdU pulse. (b, c) ICC showing increased neuronal HuC/D-positive staining after TGFβ-treatment in E16.5- but not in E13.5-derived cells. Scale bars: 100 μm. (d) Quantification of ICC stainings as shown in (b) and (c) expressed as percentage of the total DAPI-positive cell number; untreated: white bar, TGFβ treated: grey bar. p-value: untreated versus TGFβ = 0.0243 (E13.5: n = 4; E16.5: n = 4). (e, f) Immunoblots showed enhanced expression of TGFβ ligands 1 and 2 as well as SMAD2-pS465/467 in E16.5- compared to E13.5-derived cells. Arrows indicate the 12.5 kDa and 25 kDa monomeric and dimeric forms of TGFβ2 respectively. (g, h) Quantifications of TGFβ1, TGFβ2, SMAD2 and SMAD2-pS465/467 expression levels (n = 3), depicted as normalized intensity of signals from E16.5-derived cells. Intensities from E13.5-derived cells were the control level and set to 1 as indicated by the horizontal dashed line. p-values: TGFβ1 = 0.0383, TGFβ2 = 0.0380; SMAD2-pS465/467 = 0.0162. (i) Microarray analyses obtained from E13.5- and E16.5-derived cells, treated with SB431542 and TGFβ, revealed developmental dynamics of major signalling pathways. Pathway analyses were performed using Gene ontology (GO) terms (GO:04350;TGFβ signalling, GO:0046332;SMAD binding, GO:04910;insulin signalling pathway, GO:0005520;insulin-like growth factor-binding, GO:0043560;insulin receptor substrate-binding, GO:04070;Phosphatidylinositol signalling system, GO:0005942;phosphoinositide 3-kinase-complex, GO:04150;mammalian target of rapamycin (mTOR) signalling pathway) (n = 3). (j) Immunoblotting revealed increased IGF1-signalling in E13.5-derived cells. (k, l) Quantifications of protein levels for IGF1, IGFBP3, and IGF1Rβ with different phosphorylation states (n = 3), expressed as normalized intensity as above. p-values: (k) IGF1 = 0.0014, (l) IGF1Rβ-pY1135 = 0.0002, IGF1Rβ-pY980 = 0.0030. (m) Immunoblot showed enhanced AKT activation in E16.5-derived cells (n = 3). (n) Quantification of AKT, AKT-pT308 and AKT-pS473, represented as normalized intensity as above. p-values: AKT-pT308 = 0.0444, AKT-pS473 = 0.0450. *p-value < 0.05, **p-value < 0.01, ***p-value < 0.001.

Tris-buffered saline, 0.05% Tween 20 (TBST) and incubated overnight with the primary antibody. Used antibodies and dilutions are listed in the supplement. For detection enhanced chemiluminescence or Femto solution (Thermo Scientific, Waltham, MA, USA) and LAS-ImageQuant detection systems (GE Healthcare, Little Chalfont, UK) were used. ImageJ was used for densitometric quantifications.

Statistics

Analysis was performed using unpaired Student's *t*-test. Data collected as replicates are represented as the mean ± SEM for immunoblots and immunocytochemical countings.

RESULTS

TGFβ- and IGF-signalling activities are different in E13.5- and E16.5-derived cortical cells

Up to E13.5 during mouse cortical development, progenitors mainly undergo proliferation, whereas subsequent embryonic stages are dominated by neuronal and glial differentiation. To elucidate the dynamics in the developmental program of cortical cells, we tested if TGFβ induces differentiation of cultured cortical cells from E13.5, as we have recently described for E16.5-derived cells (Vogel *et al*. 2010). It is of note that cortical cells *in vitro* might respond differently to developmental stimuli compared to the natural *in vivo* situation and that the *in vitro* setting does not reflect exactly the cellular state *in vivo*. However, as we have shown recently, *in vivo* studies of TGFβ2/TGFβ3 double mutant mice corroborated our *in vitro* findings (Vogel *et al*. 2010). For this reason we chose similar culture conditions within this study to compare cytokine functions on cells derived from different developmental time points.

TGFβ induced the neuronal marker HuC/D in E16.5- but not in E13.5-derived cells (Fig. 1b–d). We tested the endogenous expression of TGFβ ligands, TGFβ receptors type I and II (TGFBR1, TGFBR2) and phosphorylation of SMAD2 and SMAD3. We found that TGFβ1 and TGFβ2 were moderately induced at E16.5 (Fig. 1e). Phosphorylation of SMAD2-S465/467 was also increased at E16.5 (Fig. 1f). Quantification of immunoblots is shown in Fig. 1g, h. Thus, TGFβ-signalling is increased and specifically required for differentiation of cortical progenitors derived from E16.5 forebrains, raising the question as to which growth factor drives proliferation and/or differentiation at E13.5. We performed a comparative microarray analysis of cortical cells at both developmental time points. Components of the IIS pathway comprised the largest fraction of developmentally regulated signalling pathways (Fig. 1i, Table S1). We next tested expression and activation of IIS components at the protein level. Expression of IGF1 was strongly increased at E13.5 as compared to E16.5 (Fig. 1j, k). Phosphorylation of IGF1-receptor β (IGF1Rβ) at residues T980 and T1135 was also induced, reflecting higher IGF1Rβ activity at E13.5 (Fig. 1j, l). We further com-

pared AKT phosphorylation at T308 (PDK1 substrate site) and S473 (mTORC2 substrate site) in E13.5 and E16.5 untreated cultured cells. Both phosphorylation events were present at E13.5, and induced at E16.5 (Fig. 1m, n). Given that IIS was induced in cultured E13.5 cells, whereas TGFβ-signalling was induced in cultured E16.5 cells, we hypothesized that IGF1 or TGFβ, respectively, might dominate AKT activation on either day of development.

IGF1 induces cortical cell proliferation, survival and differentiation specifically in E13.5-derived cells via AKT and the two mTOR complexes

We investigated the requirement of IIS for cortical cell differentiation and/or proliferation in E13.5- and E16.5-derived cells respectively. Treatment of E13.5 cortical cells with IGF1 increased the expression of the neuronal marker HuC/D, whereas the presence of the IGF1R inhibitor PPP decreased the number of differentiated neurons (Fig. 2a, c). No changes were observed in E16.5-derived cells (Fig. 2b, c). We subsequently used RTCA to assess proliferation as well as survival of cortical cells. We found that PPP inhibited cortical cell proliferation and survival of E13.5-derived cells (Fig. 2d), consistent with existing literature (Vogel 2013), but did not affect E16.5 cells (Fig. 2d). As shown by immunoblotting, IGF1 and IGF2 specifically induced the PDK1 target site AKT-pT308 and the mTORC2 substrate site AKT-pS473 in E13.5 (Fig. 2e, f, h, i), but hardly activated AKT in E16.5 cells (Fig. 2e, g, h, j). mTORC1-dependent phosphorylation of p70-S6K-pT389 and PRAS40-pS183 did not increase after exposure to IGF in E13.5 and E16.5 cells (Fig. 2e–j). At the receptor level, IGF1 induced IGF1Rβ phosphorylation at T980 and T1135 specifically in E13.5 cells. PPP-treatment slightly induced the inhibitory IRS1-S636/639 phosphorylation [negative-feedback loop (NFL), target site for p70-S6K] specifically in E13.5-, but not in E16.5-derived cells (Fig. 2h, i, j). PPP at E13.5 did not affect AKT-pT308 and -pS473 (Fig. 2h, i), which was presumably because of a low steady-state activity of AKT, as AKT strongly responded to acute IGF1 stimulation. We conclude that the PDK1-AKT-mTORC2 network responds to IGF and the IGF1Rβ at E13.5, but only weakly, if at all, at E16.5. Furthermore, IGF1 influences cortical cell proliferation, survival and differentiation in E13.5-, but not in E16.5-derived cells.

AKT, mTORC1 and mTORC2 are required for proliferation and survival of E13.5 and E16.5 cortical cells and AKT- or mTORC-inhibitors sensitize the cells to IGF1R inhibition

Next, we tested if AKT and the mTOR complexes were required for cortical cell proliferation and survival of E13.5- and E16.5-derived cells using RTCA for 72 h. Indeed, in this time interval the AKT-inhibitor MK-2206, Rapamycin and Torin1

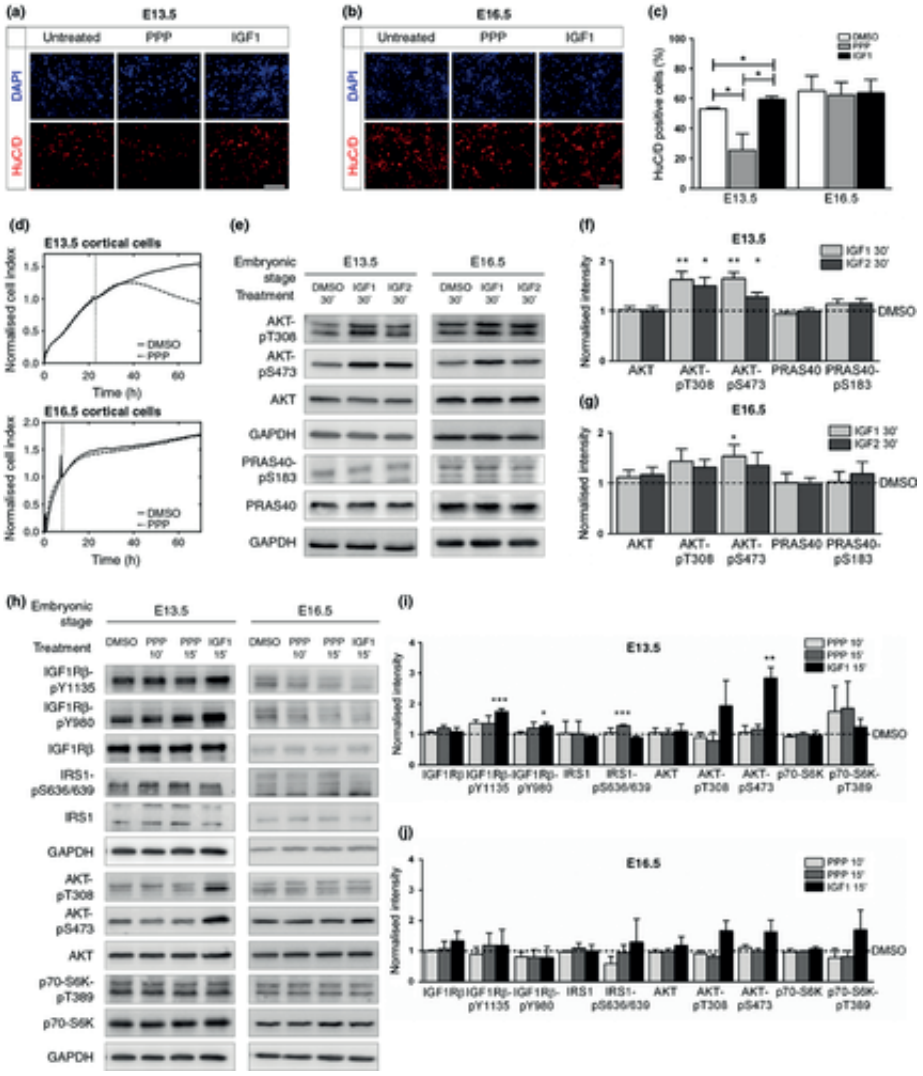
(a)
E13.5
Untreated
PPP
IGF1
DAPI
H2CD
(b)
E16.5
Untreated
PPP
IGF1
DAPI
H2CD
(c)
H2CD positive cells (%)
DMSO
PPP
IGF1
E13.5
E16.5
(d)
E13.5 cortical cells
Normalised cell index
DMSO
PPP
Time (h)
E16.5 cortical cells
Normalised cell index
DMSO
PPP
Time (h)
(e)
Embryonic stage
Treatment
E13.5
E16.5
DMSO 30'
IGF1 30'
IGF2 30'
AKT-pT308
AKT-pS473
AKT
GAPDH
PRAS40-pS183
PRAS40
GAPDH
(f)
E13.5
IGF1 30'
IGF2 30'
Normalised intensity
DMSO
AKT
AKT-pT308
AKT-pS473
PRAS40
PRAS40-pS183
(g)
E16.5
IGF1 30'
IGF2 30'
Normalised intensity
DMSO
AKT
AKT-pT308
AKT-pS473
PRAS40
PRAS40-pS183
(h)
Embryonic stage
E13.5
E16.5
Treatment
DMSO
PPP 10'
PPP 15'
IGF1 15'
IGF1Rβ-pY1135
IGF1Rβ-pY980
IGF1Rβ
IRS1-pS636/639
IRS1
GAPDH
AKT-pT308
AKT-pS473
AKT
p70-S6K-pT389
p70-S6K
GAPDH
(i)
E13.5
PPP 10'
PPP 15'
IGF1 15'
Normalised intensity
DMSO
IGF1Rβ
IGF1Rβ-pY1135
IGF1Rβ-pY980
IRS1
IRS1-pS636/639
AKT
AKT-pT308
AKT-pS473
p70-S6K
p70-S6K-pT389
(j)
E16.5
PPP 10'
PPP 15'
IGF1 15'
Normalised intensity
DMSO
IGF1Rβ
IGF1Rβ-pY1135
IGF1Rβ-pY980
IRS1
IRS1-pS636/639
AKT
AKT-pT308
AKT-pS473
p70-S6K
p70-S6K-pT389

Figure 2. Insulin-like growth factor 1 (IGF1)-signalling via mammalian target of rapamycin (mTOR) complexes was increased in E13.5-derived cells and promoted cortical cell proliferation, survival and differentiation.

(a–c) Immunocytochemistry (ICC) staining and quantification showed increased numbers of HuC/D-positive cells, expressed as percentage of the total DAPI-positive cell number, after IGF1-treatment in E13.5- (n = 4), but not E16.5- derived cells (n = 3). White bar: DMSO grey bar: Picropodophyllin (PPP), black bar: IGF1. p-values: DMSO- versus PPP-treatment = 0.0453, DMSO- versus IGF1-treatment = 0.0218, PPP- versus IGF1-treatment = 0.0222. Scale bars: 100 μm. (d) RTCA of cortical cells treated with DMSO (solid line) or IGF1R-inhibitor PPP (dashed line) revealed that only E13.5-derived cells were sensitive to IGF1-signalling. The normalized cell index is shown from two technical replicates over a time interval of 72 h; dotted vertical line: time of treatment (one representative experiment shown from n = 4). (e) Immunoblots of AKT- and PRAS40-phosphorylation after 30 min DMSO-, IGF1- and IGF2-treatments revealed that IGF1 and IGF2 activated phosphoinositide-dependent protein kinase 1 (PDK1) and mTORC2, but not mTORC1 in E13.5-derived cells, and that IGF1-treatment only activated AKT-pS473 in E16.5-derived cells. (f, g) Quantification of immunoblots as representatively shown in (e) (n = 5). Given is the normalized intensity of signals from IGF1- and IGF2-treated cells. Intensities from DMSO-treated cells were chosen as control level and set to 1 as indicated by the horizontal dashed line. p-values: (f) AKT-pT308 = 0.0052 (IGF1), 0.0180 (IGF2); AKT-pS473 = 0.0012 (IGF1), 0.0193 (IGF2). (g) AKT-pS473 = 0.0436 (IGF1). (h) Immunoblots assessing IGF1-signalling via its cognate receptor, IRS1 adapter, PDK1, mTORC1 and mTORC2 after treatment with DMSO, PPP for 10 and 15 min, or IGF1 for 15 min revealed that IGF1-signalling activated mTORC2 and induced negative-feedback loop (NFL) in E13.5-derived cortical cells. (i, j) Quantifications of the proteins depicted in (h) (n = 3). Given is the normalized intensity of signals as above. p-values: (i) IGF1Rβ-pY1135 = 0.0006 (IGF1), IGF1Rβ-pY980 = 0.0336 (IGF1), IRS1-pS636/630 = 0.0010 (PPP 15 min), AKT-pS437 = 0.0062 (IGF1). *p-value < 0.05, **p-value < 0.01, ***p-value < 0.001.

interfered with cortical cell proliferation and survival at both developmental time points (Fig. 3a, b). Especially in E16.5-derived cells inhibition of both mTOR complexes through Torin1 had the strongest effect, whereas Rapamycin-treatment alone affected the cells only moderately. This finding indicated potential additive effects of both mTOR complexes. To confirm RTCA results, we performed ICC stainings upon MK-2206-, Rapamycin-, or Torin1-treatment of E16.5-derived cells at DIV6 and 8, respectively, that is in an extended time interval compared to RTCA. Assessment of proliferation via BrdU staining showed strong dependence of cell proliferation on mTORC1 and mTORC2, whereas MK-2206-mediated AKT blockage did not significantly reduce cell proliferation (Fig. 3c, d). Similarly, blocking mTORC1 and mTORC2 resulted in increased numbers of cells positive for the apoptosis marker activated Caspase 3 (aCASP3), whereas prolonged AKT inhibition did not induce apoptosis (Fig. 3e, f). These results show the requirement of both mTOR complexes for cell survival independent of the treatment paradigm.

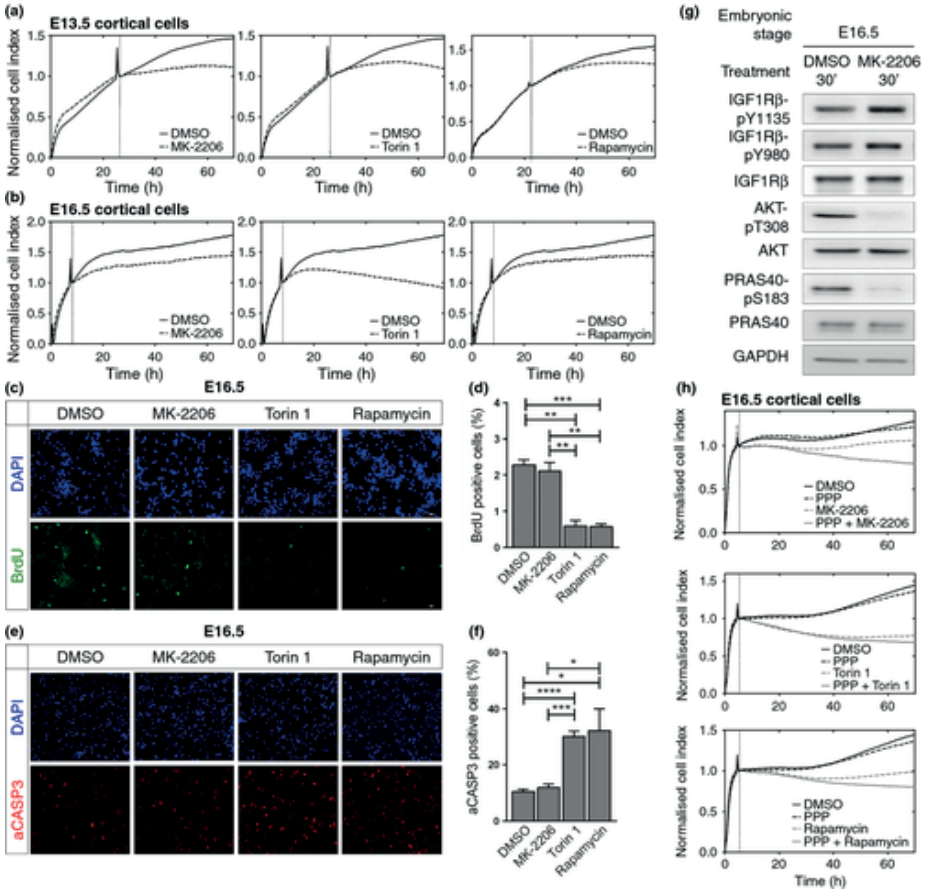
(a)
E13.5 cortical cells
Normalised cell index
Time (h)
DMSO
MK-2206
Torin 1
Rapamycin
(b)
E16.5 cortical cells
(c)
E16.5
DMSO
MK-2206
Torin 1
Rapamycin
DAPI
BrdU
(d)
BrdU positive cells (%)
(e)
aCASP3
(f)
aCASP3 positive cells (%)
(g)
Embryonic stage
E16.5
Treatment
DMSO 30'
MK-2206 30'
IGF1Rβ-pY1135
IGF1Rβ-pY980
IGF1Rβ
AKT-pT308
AKT
PRAS40-pS183
PRAS40
GAPDH
(h)
E16.5 cortical cells
PPP
PPP + MK-2206
PPP + Torin 1
PPP + Rapamycin

Figure 3. AKT, mTORC1 and mTORC2 were required for proliferation and survival of E13.5 and E16.5 cortical cells, and AKT- or mTOR-inhibitors sensitized the cells to IGF1R-inhibition.
(a–b) RTCA of E13.5 and E16.5-derived cortical cells treated with DMSO (solid line) or inhibitors (dashed lines) revealed that proliferation of E13.5- and E16.5-derived cortical cells depended on active AKT- and mTOR-signalling, AKT-inhibitor MK-2206, mTORC1/mTORC2-inhibitor Torin1, and mTORC1-inhibitor Rapamycin. Data are shown as in Fig. d (one representative experiment shown from n = 3). (c) Immunocytochemistry stainings for BrdU after a 60 min pulse revealed that blockage of mTORC1 and mTORC2, but not AKT led to reduced proliferation. Scale bar: 100 μm. (d) Quantification of BrdU stainings, expressed as percentage of the total DAPI-positive cell number (n = 3). p-values: DMSO versus Torin1 = 0.0013, MK2206 versus Torin1 = 0.0056, DMSO versus Rapamycin = 0.0004, MK2206 versus Rapamycin = 0.0032. (e) Immunocytochemistry stainings for detection of aCASP3 in E16.5-derived cortical cells treated with MK-2206, Torin1 and Rapamycin revealed that inhibition of AKT- and mTOR complexes led to apoptosis at E16.5. Scale bar: 100 μm. (f) Quantification of aCASP3-positive cells shown in (e) (n = 4). p-values: DMSO versus Rapamycin = 0.0316, DMSO versus Torin1 < 0.0001, MK-2206 versus Torin1 = 0.0002, MK-2206 versus Rapamycin = 0.0415. (g). Immunoblot of proteins from E16.5-derived cortical cells after treatment for 30 min with DMSO or AKT-inhibitor MK-2206 revealed reduced mTORC1 activity and subsequent negative-feedback loop (NFL) suppression. (h) RTCA revealed that AKT- and mTORC-inhibitors sensitized E16.5-derived cortical cells to IGF1R inhibition. Black solid line: DMSO-treatment, black dashed line: Picropodophyllin (PPP)-treatment, grey dashed line MK-2206-, Torin1- or Rapamycin-treatment, respectively, grey solid line: PPP- and MK-2206-, PPP- and Torin1-, PPP- and Rapamycin-co-treatments respectively. The normalized cell index is shown as above (one representative experiment shown from n = 3). *p-value < 0.05, **p-value < 0.01, ***p-value < 0.001.

As we observed that AKT-mTORC1- and mTORC2-networks are required for cell growth of E16.5-derived cells although IGF1 and IGF1Rβ were not, we analysed the effect of AKT inhibition by MK-2206 in cortical cells on network activities specifically at E16.5 by immunoblotting. As expected, we found that mTORC1 was inhibited by MK-2206, as monitored by its readout PRAS40-pS183 (Fig. 3g). Notably, we found that the IGF1Rβ became moderately activated upon AKT inhibition, which may be caused by NFL suppression of IGFR-signalling (Laplante and Sabatini 2012) in response to reduced mTORC1 activity. Therefore, we hypothesized that inhibition of AKT- or the mTOR complexes might sensitize E16.5 cortical cells to the IGF1R-inhibitor PPP. Indeed, we found that PPP in combination with MK-2206, Rapamycin, or Torin1 blocked proliferation and survival of E16.5 cortical cells (Fig. 3h), although PPP alone did not have an inhibitory effect (Fig. 2b–d). We conclude that IGF1 does not promote cortical cell proliferation and survival at the later, neurogenic developmental stage (E16.5), but under conditions of AKT or mTOR inhibition, IGF1 sensitivity can be reintroduced into the system. Furthermore, cell proliferation and survival

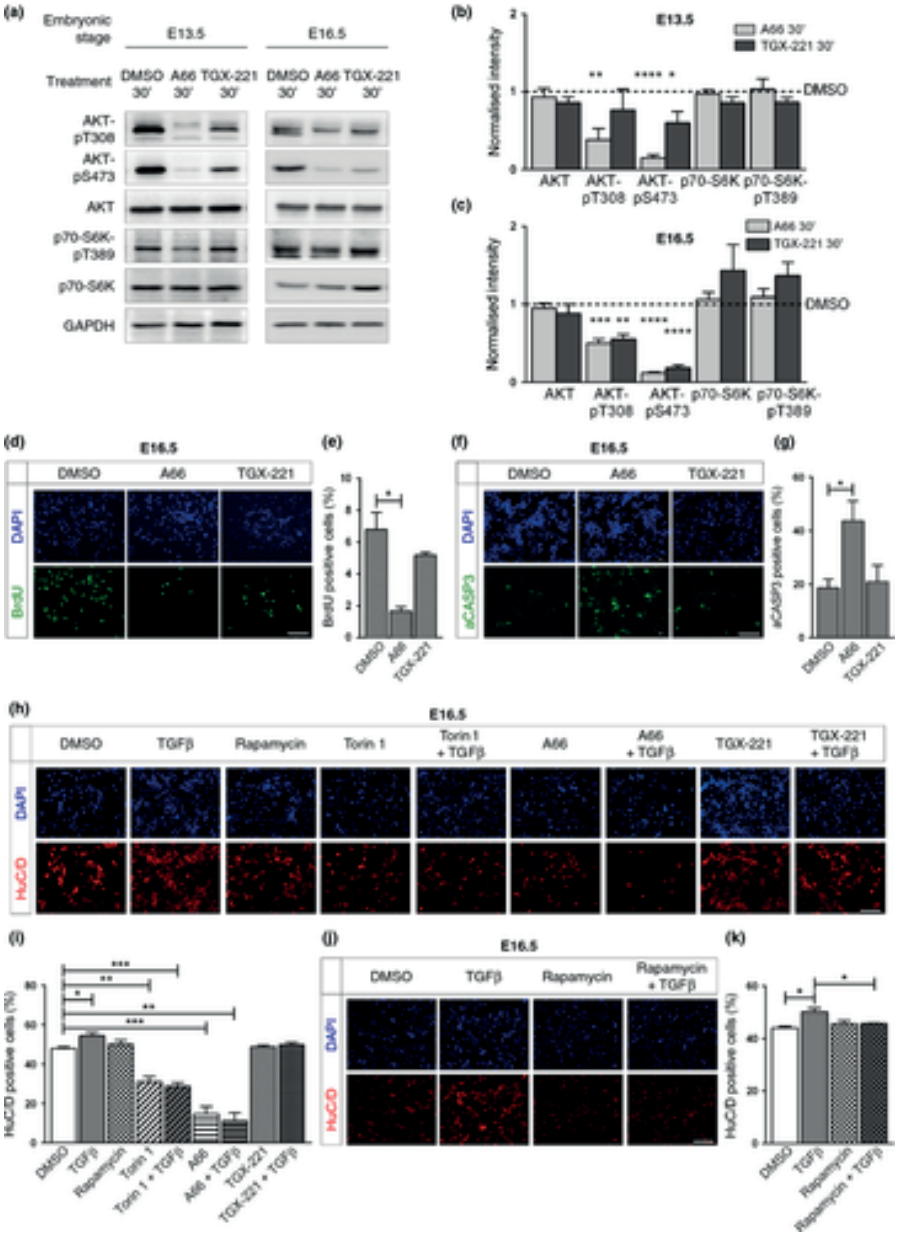
(a)
Embryonic stage
E13.5
E16.5
Treatment
DMSO 30'
A66 30'
TGX-221 30'
AKT-pT308
AKT-pS473
AKT
p70-S6K-pT389
p70-S6K
GAPDH
(b)
E13.5
A66 30'
TGX-221 30'
Normalised intensity
DMSO
AKT
AKT-pT308
AKT-pS473
p70-S6K
p70-S6K-pT389
(c)
E16.5
(d)
E16.5
DMSO
A66
TGX-221
DAPI
BrdU
(e)
BrdU positive cells (%)
(f)
E16.5
aCASP3
(g)
aCASP3 positive cells (%)
(h)
E16.5
DMSO
TGFβ
Rapamycin
Torin 1
Torin 1 + TGFβ
A66
A66 + TGFβ
TGX-221
TGX-221 + TGFβ
HuC/D
(i)
HuC/D positive cells (%)
(j)
E16.5
Rapamycin + TGFβ
(k)
HuC/D positive cells (%)

Figure 4. PI3K-p110-alpha and -beta had similar specificities towards mammalian target of rapamycin (mTOR) complex activation but distinct influence on the proliferative and survival response of E16.5-derived cortical progenitors.
(a) Immunoblots of E13.5- and E16.5-derived proteins after cells were treated (30 min) with DMSO, A66 or TGX-221 revealed that PI3K-p110-alpha activated phosphoinositide-dependent protein kinase 1 (PDK1) and mTORC2 in E13.5- and E16.5-derived cells, whereas PI3K-p110-beta activated mTORC2 at both developmental time points, but PDK1 only in E16.5-derived cortical cells. (b, c) Quantification of immunoblots as shown in (a) (E13.5: n = 5, E16.5: n = 3), expressed as normalized intensity compared to DMSO control that was set to 1 (horizontal dashed line). p-values: E13.5: AKT-pT308 = 0.0026 (A66), AKT-pS473 = ****p < 0.0001 (A66), 0.0231 (TGX-221); E16.5: AKT-pT308 = 0.0008 (A66), 0.0014 (TGX-221), AKT-pS473 ****p ≤ 0.0001 (A66), ****p < 0.0001 (TGX-221). (d) Immunocytochemistry (ICC) stainings for BrdU after a 60 min pulse revealed that blocking PI3K-p110-alpha but not -beta hampered proliferation of E16.5-derived cells. Scale bar: 100 μm. (e) Quantification of BrdU-positive per total DAPI-positive cells after interference with PI3K-signalling (n = 3). p-value: DMSO versus A66 = 0.0102. (f) ICC stainings of E16.5-derived cortical for aCASP3 revealed that in contrast to TGX-221 A66-treatment induced apoptosis. Scale bar: 100 μm. (g) Quantification of aCASP3-positive cells referred to the total DAPI-positive cell number (n = 5). p-value: DMSO versus A66 = 0.0149. (h) ICC stainings for HuC/D after single and combined treatments for TGFβ, PI3K-subunit and mTORC inhibitors indicated that TGFβ, different PI3K isoforms and mTORC2 mediate neuronal differentiation of E16.5-derived cells. Scale bar: 100 μm. (i) Quantification of HuC/D-positive per total DAPI-positive cells after treating with different combinations of inhibitors and TGFβ (n = 3). p-values: DMSO versus TGFβ = 0.0316, DMSO versus Torin1 = 0.0034, DMSO versus Torin1 + TGFβ = 0.0008, DMSO versus A66 = 0.0010, DMSO versus A66 + TGFβ = 0.0010. (j–k) ICC and quantification of E16.5-derived cells stained for HuC/D after treatment with TGFβ, Rapamycin and combination of both, which were performed in different biological sets as experiments represented in Fig. i (n = 3) Scale bars: 100 μm. p-values: DMSO versus TGFβ = 0.0163, TGFβ versus Rapamycin + TGFβ = 0.0336. *p-value < 0.05, **p-value < 0.01, ***p-value < 0.001.

is influenced by active AKT and the two mTOR complexes at both, mitotic and neurogenic developmental stages.

PI3K-p110-alpha and -beta, but not TGFβ, are required for activation of mTORC2 substrates in cortical cells

IGF1-signalling induced AKT-mTORC1/mTORC2-dependent proliferation and survival exclusively in E13.5-derived cells (Fig. 2), but we observed even greater phosphorylation of AKT in E16.5 cells (Fig. 1m, n). We next investigated whether TGFβ might be responsible for AKT-mTORC1/mTORC2 activation in the later development stage E16.5. TGFβ was a strong candidate, as we had found that TGFβ induced differentiation in E16.5 cells (Fig. 1c, d), and TGFβ1 and TGFβ2 expression as well as SMAD2 phosphorylation were induced at this neurogenic stage (Fig. 1e–h). However, in E13.5- as well as E16.5-derived cells,

TGFβ- or SB431542-treatment neither influenced AKT nor the two mTOR complexes (Figure S1).

We extended our analyses to different PI3K isoforms as these are strong candidates for differential mTOR complex activation and our data indicated that interference with both mTORC1 and mTORC2 by Torin1 exhibited a stronger effect than interference by the more mTORC1 selective drug Rapamycin alone (Fig. 3a, b). We treated cortical cells from E13.5 and E16.5 forebrains with the PI3K-p110-alpha-specific inhibitor A66, or with the PI3K-p110-beta-specific inhibitor TGX-221. The PI3K-p110-alpha inhibitor A66 ablated AKT-T308 phosphorylation (PDK1 target site) in cells derived from early, mitotically dominated developmental stage (E13.5) and in the more differentiative stage (E16.5) (Fig. 4a–c). However, A66 did not inhibit the mTORC1 readout p70-S6K-pT389. In contrast, A66 inhibited the mTORC2-readout AKT-pS473 in cells derived from both developmental time points (Fig. 4a–c). Treatment with PI3K-p110-beta inhibitor TGX-221 inactivated PDK1-dependent AKT-pT308 only in E16.5 cells, but the mTORC2-specific readout AKT-pS473 was inhibited at both developmental stages (Fig. 4a–c). TGX-221 did not inhibit the mTORC1-specific readout p70-S6K-pT389. We conclude that PI3K-p110-alpha and beta inhibition mainly affects mTORC2-signalling in cortical cells. Interference with mTORC2-signalling is stronger in cortical cells of later than of earlier developmental stages.

Our RTCA data (Fig. 3a, b) indicated that mTORC2 might be of importance for proliferation and survival at E16.5. These results and the strong inactivation of mTORC2 observed by immunoblotting led us to the hypothesis, that inhibition of PI3K-subtype-signalling should have similar phenotypic consequences as inhibition of either mTOR complex. To investigate this hypothesis, we analysed cortical cell proliferation and survival at E16.5 upon PI3K-p110-alpha or -beta inhibition with A66 or TGX-221. A66 inhibited proliferation of E16.5 cells (Fig. 4d, e). Interestingly, the PI3K-p110-beta inhibitor TGX-221 did not influence cortical cell proliferation at the neurogenic stage (E16.5) (Fig. 4d, e). We assessed cell survival by detecting activated Caspase 3 and observed that blocking of PI3K-p110-alpha activity strongly induced apoptosis (Fig. 4f, g). In contrast, the cells survived loss of PI3K-p110-beta activity (Fig. 4f, g). Thus, although network activities on AKT were comparable for inhibition of either PI3K isoform at this neurogenic stage, the inhibitors elicited different phenotypic responses. Thereby, the PI3K-p110-alpha inhibitor mimicked the suppression of proliferation and survival by Torin1 (but not rapamycin) in E16.5-derived cells.

We next studied the implication of different PI3K isoforms and mTOR complex activities on neuronal differentiation in relation to TGFβ in E16.5-derived cells. HuC/D immunostaining revealed (Fig. 4h–k) that TGFβ induced neuronal differentiation of E16.5 cells, and Torin1-treatment reduced the numbers of neurons even below those in control cells (Fig. 4h, i). In contrast, Rapamycin alone did not affect neuron numbers (Fig. 4j, k). Blocking of PI3K-p110-alpha activity reduced neuron numbers to a similar extent as Torin1, whereas reduced PI3K-p110-beta alone did not interfere with appearance of HuC/D-positive neurons (Fig. 4h, i). Co-treatments with TGFβ showed that both Torin1 and Rapamycin abolished the ability of TGFβ to induce neuronal differentiation (Fig. 4h–k). Taking all these data together, we conclude that mTORC2 is a major driver of proliferation and survival of E16.5-derived cortical cells, and is under control of PI3K-p110-alpha-signalling; both mTOR complexes are required for TGFβ-dependent differentiation. Thus, PI3K-mTORC1/mTORC2 activity is required to mediate the cellular competence to induce neuronal differentiation upon presence of exogenous TGFβ.

DISCUSSION

In this study, we show firstly that TGFβ promotes neuronal differentiation of cortical progenitors exclusively in the later, differentiative stage (E16.5) but not in a stage when mitosis dominates (E13.5) (Fig. 1b–d). Furthermore, IGF1-treatment of cortical cells results in increased proliferation, survival and differentiation exclusively in E13.5- but not E16.5-derived cells (Fig. 2a–d). Second, we show that in E16.5-derived cells mTORC2 has a central role in promoting survival, proliferation as well as neuronal differentiation (Fig. 3b–f, h, Fig. 4h–k), although contribution of rapamycin-insensitive mTORC1 effectors cannot be excluded (Thoreen and Sabatini 2009; Thoreen *et al.* 2009; Kang *et al.* 2013). mTORC2 promoted survival, proliferation and differentiation is also under control of PI3K-p110-alpha-signalling. PI3K-p110-beta-signalling activates mTORC2 in E16.5-derived cells, but this does not lead to changes in cell survival, proliferation and differentiation (Fig. 4a–i). mTOR activation is independent of either IGF1 or TGFβ. However, the PI3K-mTORC1/mTORC2 pathway needs to be active for TGFβ-mediated neuronal differentiation (Fig. 4h–k).

Our study shows that TGFβ and IGF1 are both involved in regulating cortical cell development. Thereby, the two signalling pathways exert different functions that are confined to two distinct developmental time points: cell proliferation, survival and neuronal differentiation during early development is under the influence of IGF1, cell differentiation at later developmental time points is under the control

of TGFβ. Although there are generally multiple points of intersection between the two signalling pathways, our data show that in cortical development there is a temporal separation of TGFβ- and IGF1-signalling. Thus, our data reflect that in cortical cells one pathway is dominant over the other at specific developmental time points. Of course, our findings do not exclude that direct cross-talk between the two pathways exists in addition.

The question that arises from our observations is why the signalling mechanisms differ between E13.5- and E16.5-derived cells. Our data support the model that this is mainly owing to differences in ligand expression and availability, but not because of different expression levels of the receptors. While the latter are expressed in comparable amounts, expression of TGFβ1 and TGFβ2 rises significantly in later, neurogenic E16.5-derived cells, whereas IGF1 expression declines. Alongside, we also observe less activation of the IGF1Rβ, which might be a consequence of lower amounts of available ligands. However, other mechanisms are also likely and might act in parallel. Possible mechanisms are changes in ligand affinity at the receptor level or altered composition of intracellular receptor adapter proteins that lead to different pathway activation capacities. It might also be likely that the number of active pathways increases with development and that multiple pathways compete for down-stream signals such as mTORC.

An increasing body of evidence supports the regulation of PI3K-, AKT- and the mTOR-network also by TGFβ (Bakin *et al.* 2000; Conery *et al.* 2004; Remy *et al.* 2004; Song *et al.* 2006; Lamouille *et al.* 2012; Xue *et al.* 2012; Zhang *et al.* 2012). However, TGFβ does not activate mTOR-signalling in cortical cells under the conditions that we applied in this study. We reported earlier that TGFβ-mediated neuronal differentiation is dependent on SMAD-signalling (Vogel *et al.* 2010). In addition to this predominant signalling pathway, this study implies that TGFβ required basal mTOR activity to promote neuronal differentiation. Whether this finding reflects a novel molecular intersection, or rather an indirect dependence on a general cellular function, for example protein synthesis, awaits further investigation. Our data indicate that in E16.5-derived cortical cells, activation of the mTOR network is neither under control of IGF1 nor of TGFβ. However, other studies report on the activation of the mTOR network during CNS development through various extrinsic stimuli, emphasizing the central role of mTOR in controlling proliferation as well as differentiation. EGF and FGF2 activate PI3K as well as mTORC1 and support maintenance of self-renewal capacities of neural progenitor cells (Peltier *et al.* 2007; Sato *et al.* 2010). Proliferation of neural progenitors of different origins, for example from the embryonic cerebral cortex or

adult hippocampus, is also under control of endocannabinoids that signal via the CB2 cannabinoid-receptor and mTORC1 (Palazuelos *et al*. 2012). Mature hippocampal neurons activate the mTORC1 network upon exposure to activity released vascular endothelial growth factor (Kim *et al*. 2008). These results might establish a link between mTORC1 activity and synaptic plasticity. Growth and branching of dendrites of hippocampal neurons is under control of REELIN that activates the mTOR complexes in this context (Jossin and Goffinet 2007). Brain-derived neurotrophic factor activates mTOR complexes and thereby regulates protein synthesis in cortical neurons. This pathway is also under control of the cellular energy sensor AMP-dependent kinase. AMP-dependent kinase is active in conditions of insufficient nutrients, such as low glucose, and interferes with brain-derived neurotrophic factor-mediated mTOR activation (Ishizuka *et al*. 2013). mTOR complexes are as well affected through WNT-signalling in the CNS, whereby glycogen synthase kinase-3 beta acts as negative regulator of mTOR in synaptic plasticity (Ma *et al*. 2011). Together this data not only reinforces the importance of mTOR-signalling but also the diversity of its activation.

The mTOR complexes have been implicated in proliferation as well as differentiation of telencephalic cells, while survival seems to be independent of mTORC1 (Aberg *et al*. 2003; Sinor and Lillien 2004; Peltier *et al*. 2007; Han *et al*. 2008b). In continuation of these studies our data dissect mTORC1 and mTORC2 substrate activation in the cerebral cortex. Although IGF1-AKT-mTOR-signalling has been studied in this cellular context, most analyses did not investigate the pathways down-stream of AKT and exclusively used Rapamycin. In this study, we show that both mTOR complexes control proliferation in cells derived from two different developmental time points, E13.5 as well as E16.5. This notion that mTORC2 specifically contributes to the observed effects, comes from the observation that we hardly saw activation of mTORC1 substrates such as PRAS40 or p70-S6K, whereas mTORC2 substrate AKT-pS473 was consistently regulated in our immunoblots. Furthermore, our study indicates that Torin1-sensitive mTORC2 activity and/or Rapamycin-insensitive mTORC1 are required for neuronal differentiation, whereas proliferation and survival are equally affected by Torin1 and Rapamycin.

Regulation up-stream of mTORC1 and mTORC2 is an emerging field of interest and we thus studied the role of the mTORC1 activator AKT. We observed that AKT inhibition using MK-2206 did not result in the same cellular response of decreased proliferation and increased apoptosis in prolonged treatments as Torin1. Further, RTCA analyses revealed a milder effect of MK-2206 than

for Torin1, suggesting that the Torin1 effects are mTORC2 specific, and that AKT is not the mTORC2 effector with regard to proliferation in E16.5 cortical cells. As different variants have been suggested to separately activate the two mTOR complexes (Dalle Pezze *et al*. 2012), we studied two PI3K-p110 isoforms. PI3K-p110-alpha inhibition mimicked Torin1-mediated interference with regard to cell proliferation, survival and neuronal differentiation, and mainly affected phosphorylation of mTORC2 substrates. In contrast, PI3K-p110-beta inhibition also affected mTORC2 substrate phosphorylation, but did not result in observable cellular phenotypes. This suggests that E16.5-derived cortical cells have different mTORC2-subtypes that may be differentially modulated through different PI3K-p110 isoforms. Several studies indicate that this interpretation is a very likely scenario, as different mSIN1 isoforms (Frias *et al*. 2006) and phosphorylation states (Liu *et al*. 2013) as well as different posttranslational modifications of RICTOR (Julien *et al*. 2010; Chen *et al*. 2011; Glidden *et al*. 2012) have been reported. It is of course also possible that further, unidentified factors associate or co-signal with mTORC2.

Differential effects of PI3K-p110-alpha and p110-beta have been reported in myoblasts (Matheny and Adamo 2010; Matheny *et al*. 2012) and hypothalamic neurons (Al-Qassab *et al*. 2009). Thus, the divergence of signals at the level of PI3K-subunits upon cytokine stimulation is of general importance. Few data report so far on PI3K-p110-subtype-specific functions in the CNS and no data are available on specific functions of PI3K-p110-alpha and -beta in the context of development of the cerebral cortex. Although ablation of PI3K-p110-alpha is embryonic lethal in mice, data indicate a proliferative function of this subunit in early CNS development (Bi *et al*. 1999), corroborating our findings.

In this study, we have interfered with the mTOR complexes and PI3K-isoforms-p110-alpha and p110-beta by pharmacological inhibition. This allowed us to study the implications of these proteins in primary cortical cells, for which owing to low cell numbers, low transfection and transduction efficiencies it is technically demanding to use other techniques of intervention. Especially the finding that PI3K-p110-alpha inhibition mimicks phenotypically the effects of Torin1, whereas PI3K-p110-beta inhibition does not, underscores the notion of diverging signalling cascades at the level of PI3K. The inhibitor based finding that the p110-alpha- and p110-beta-PI3K isoforms affect mTORC2 substrates in cortical cells is intriguing and will be further explored in the future by alternative techniques including measurement of PI3K-subunit activities, and RNA knockdown

approaches; the latter can also help to further dissect the relative contribution of either mTOR complex.

Acknowledgements and conflict of interest disclosure

The authors thank Dr. C. Hindley, Department of Molecular Embryology, for editing the English phrasing of this manuscript. This study was supported in part by EC 6th FP NoE LifeSpan (LSHG-CT-2007-036894, KT), Schlieben-Lange-Programm (KT), BMBF GerontoSys II – NephAge (031 5896A, KT), a Rosalind-Franklin-Fellowship of the University of Groningen, NL (KT), Stiftung der Deutschen Wirtschaft (NH), German Research Foundation DFG (TV, KK), the Excellence Initiative of the German Research Foundation (EXC 294, KT; GSC-4, Spemann Graduate School, MTP), Freiburg Institute for Advanced Studies FRIAS Junior Fellowship (KT).

SDW, MTP, SCW, NH, RV and CK planned, conducted, and analysed experiments. KT and TV planned and guided the experiments and project, analysed and interpreted the data, wrote the article, and approved together with JT and KK the final version to be published.

All experiments were conducted in compliance with the ARRIVE guidelines. The authors have no conflict of interest to declare.

REFERENCES

Aberg M. A. I., Aberg N. D., Palmer T. D. *et al.* (2003) IGF-I has a direct proliferative effect in adult hippocampal progenitor cells. Mol. Cell. Neurosci. 24, 23–40.

Ajo R., Cacicedo L., Navarro C. and Sánchez-Franco F. (2003) Growth hormone action on proliferation and differentiation of cerebral cortical cells from fetal rat. Endocrinology 144, 1086–1097.

Al-Qassab H., Smith M. A., Irvine E. E. *et al.* (2009) Dominant role of the p110beta isoform of PI3K over p110alpha in energy homeostasis regulation by POMC and AgRP neurons. Cell Metab. 10, 343–354.

Arsenijevic Y. and Weiss S. (1998) Insulin-like growth factor-I is a differentiation factor for postmitotic CNS stem cell-derived neuronal precursors: distinct actions from those of brain-derived neurotrophic factor. J. Neurosci. 18, 2118–2128.

Bakin A. V., Tomlinson A. K., Bhowmick N. A., Moses H. L. and Arteaga C. L. (2000) Phosphatidylinositol 3-kinase function is required for transforming growth factor beta-mediated epithelial to mesenchymal transition and cell migration. J. Biol. Chem. 275, 36803–36810.

Bi L., Okabe I., Bernard D. J., Wynshaw-Boris A. and Nussbaum R. L. (1999) Proliferative defect and embryonic lethality in mice homozygous for a deletion in the p110alpha subunit of phosphoinositide 3-kinase. J. Biol. Chem. 274, 10963–10968.

Chen C. H., Shaikenov T., Peterson T. R., Aimbetov R., Bissenbaev A. K., Lee S. W., Wu J., Lin H. K. and Sarbassov dos D. (2011) ER stress inhibits mTORC2 and Akt signaling through GSK-3beta-mediated phosphorylation of rictor. Sci. Signal., 4, ra10.

Conery A. R., Cao Y., Thompson E. A., Townsend C. M., Jr, Ko T. C. and Luo K. (2004) Akt interacts directly with Smad3 to regulate the sensitivity to TGF-beta induced apoptosis. Nat. Cell Biol. 6, 366–372.

Dalle Pezze P., Sonntag A. G., Thien A. *et al.* (2012) Dynamic Network A Model of mTOR Signaling Reveals TSC-Independent mTORC2 Regulation. Sci. Signal., 5, ra25.

Danielpour D. and Song K. (2006) Cross-talk between IGF-I and TGF-β signaling pathways. Cytokine Growth Factor Rev. 17, 59–74.

Frias M. A., Thoreen C. C., Jaffe J. D., Schroder W., Sculley T., Carr S. A. and Sabatini D. M. (2006) mSin1 is necessary for Akt/PKB phosphorylation, and its isoforms define three distinct mTORC2s. Curr. Biol. 16, 1865–1870.

Glidden E. J., Gray L. G., Vemuru S., Li D., Harris T. E. and Mayo M. W. (2012) Multiple site acetylation of Rictor stimulates mammalian target of rapamycin complex 2 (mTORC2)-dependent phosphorylation of Akt protein. J. Biol. Chem. 287, 581–588.

Han B. H., Zhou M. l., Abousaleh F. *et al.* (2008a) Cerebrovascular dysfunction in amyloid precursor protein transgenic mice: contribution of soluble and insoluble amyloid- peptide, partial restoration via -secretase inhibition. J. Neurosci. 28, 13542–13550.

Han J., Wang B., Xiao Z., Gao Y., Zhao Y., Zhang J., Chen B., Wang X. and Dai J. (2008b) Mammalian target of rapamycin (mTOR) is involved in the neuronal differentiation of neural progenitors induced by insulin. Mol. Cell. Neurosci. 39, 118–124.

Ishizuka Y., Kakiya N., Witters L. A., Oshiro N., Shirao T., Nawa H. and Takei N. (2013) AMP-activated protein kinase counteracts brain-derived neurotrophic factor-induced mammalian target of rapamycin complex 1 signaling in neurons. J. Neurochem. 127, 66–77.

Jossin Y. and Goffinet A. M. (2007) Reelin signals through phosphatidylinositol 3-kinase and Akt to control cortical development and through mTor to regulate dendritic growth. Mol. Cell. Biol. 27, 7113–7124.

Julien L. A., Carriere A., Moreau J. and Roux P. P. (2010) mTORC1-activated S6K1 phosphorylates Rictor on threonine 1135 and regulates mTORC2 signaling. Mol. Cell. Biol. 30, 908–921.

Kang S. A., Pacold M. E., Cervantes C. L. *et al.* (2013) mTORC1 phosphorylation sites encode their sensitivity to starvation and rapamycin. Science 341, 1236566.

Kim B. W., Choi M., Kim Y. S. *et al.* (2008) Vascular endothelial growth factor (VEGF) signaling regulates hippocampal neurons by elevation of intracellular calcium and activation of calcium/calmodulin protein kinase II and mammalian target of rapamycin. Cell. Signal. 20, 714–725.

Lamming D. W., Ye L., Katajisto P. *et al.* (2012) Rapamycin-induced insulin resistance is mediated by mTORC2 loss and uncoupled from longevity. Science 335, 1638–1643.

Lamouille S., Connolly E., Smyth J. W., Akhurst R. J. and Derynck R. (2012) TGF-beta-induced activation of mTOR complex 2 drives epithelial-mesenchymal transition and cell invasion. J. Cell Sci. 125, 1259–1273.

Laplante M. and Sabatini D. M. (2012) mTOR Signaling in Growth Control and Disease. Cell 149, 274–293.

Liu P., Gan W., Inuzuka H. *et al.* (2013) Sin1 phosphorylation impairs mTORC2 complex integrity and inhibits downstream Akt signalling to suppress tumorigenesis. Nat. Cell Biol. 15, 1340–1350.

Ma T., Tzavaras N., Tsokas P., Landau E. M. and Blitzer R. D. (2011) Synaptic stimulation of mTOR is mediated by Wnt signaling and regulation of glycogen synthetase kinase-3. J. Neurosci. 31, 17537–17546.

Mairet-Coello G., Tury A. and DiCicco-Bloom E. (2009) Insulin-like growth factor-1 promotes G(1)/S cell cycle progression through bidirectional regulation of cyclins and cyclin-dependent kinase inhibitors via the phosphatidylinositol 3-kinase/Akt pathway in developing rat cerebral cortex. J. Neurosci. 29, 775–788.

Matheny R. W., Jr and Adamo M. L. (2010) PI3K p110 alpha and p110 beta have differential effects on Akt activation and protection against oxidative stress-induced apoptosis in myoblasts. Cell Death Differ. 17, 677–688.

Matheny R. W., Lynch C. M. and Leandry L. A. (2012) Enhanced Akt phosphorylation and myogenic differentiation in PI3K p110 beta-deficient myoblasts is mediated by PI3K p110 alpha and mTORC2. Growth Factors 30, 367–384.

Palazuelos J., Ortega Z., Diaz-Alonso J., Guzman M. and Galve-Roperh I. (2012) CB2 cannabinoid receptors promote neural progenitor cell proliferation via mTORC1 signaling. J. Biol. Chem. 287, 1198–1209.

Peltier J., O'Neill A. and Schaffer D. V. (2007) PI3K/Akt and CREB regulate adult neural hippocampal progenitor proliferation and differentiation. Dev. Neurobiol., 67, 1348–1361.

Remy I., Montmarquette A. and Michnick S. W. (2004) PKB/Akt modulates TGF-beta signalling through a direct interaction with Smad3. Nat. Cell Biol. 6, 358–365.

Sarbassov D. D., Ali S. M., Sengupta S., Sheen J. H., Hsu P. P., Bagley A. F., Markhard A. L. and Sabatini D. M. (2006) Prolonged rapamycin treatment inhibits mTORC2 assembly and Akt/PKB. Mol. Cell 22, 159–168.

Sato A., Sunayama J., Matsuda K.-I., Tachibana K., Sakurada K., Tomiyama A., Kayama T. and Kitanaka C. (2010) Regulation of neural stem/progenitor cell maintenance by PI3K and mTOR. Neurosci. Lett. 470, 115–120.

Siegenthaler J. A. and Miller M. W. (2008) Generation of Cajal-Retzius neurons in mouse forebrain is regulated by transforming growth factor β-Fox signaling pathways. Dev. Biol. 313, 35–46.

Sinor A. D. and Lillien L. (2004) Akt-1 expression level regulates CNS precursors. J. Neurosci. 24, 8531–8541.

Song K., Wang H., Krebs T. L. and Danielpour D. (2006) Novel roles of Akt and mTOR in suppressing TGF-beta/ALK5-mediated Smad3 activation. EMBO J. 25, 58–69.

Sonntag A. G., Dalle Pezze P., Shanley D. P. and Thedieck K. (2012) A modelling-experimental approach reveals IRS dependent regulation of AMPK by Insulin. FEBS J. 279, 3314–3328.

Takahashi T., Nowakowski R. S. and Caviness V. S. (1996) The leaving or Q fraction of the murine cerebral proliferative epithelium: a general model of neocortical neuronogenesis. J. Neurosci. 16, 6183–6196.

Thoreen C. C. and Sabatini D. M. (2009) Rapamycin inhibits mTORC1, but not completely. Autophagy 5, 725–726.

Thoreen C. C., Kang S. A., Chang J. W. *et al*. (2009) An ATP-competitive mammalian target of rapamycin inhibitor reveals rapamycin-resistant functions of mTORC1. J. Biol. Chem. 284, 8023–8032.

Urbanska M., Gozdz A., Swiech L. J. and Jaworski J. (2012) Mammalian target of rapamycin complex 1 (mTORC1) and 2 (mTORC2) control the dendritic arbor morphology of hippocampal neurons. J. Biol. Chem. 287, 30240–30256.

Vogel T. (2013) Insulin/IGF-signalling in embryonic and adult neural proliferation and differentiation in the mammalian central nervous system, in Trends in Cell Signaling Pathways in Neuronal Fate Decision (Wislet-Gendebien S., ed.), pp. 37–73. InTech Open Access System, Rijeka, Croatia.

Vogel T., Ahrens S., Buttner N. and Krieglstein K. (2010) Factor transforming growth cell promotes neuronal fate of cortical mouse and in hippocampal progenitors vitro and vivo in: identification of Nedd9 as an component essential signaling. Cereb. Cortex (New York N.Y.: 1991), 20, 661–671.

Xue G., Restuccia D. F., Lan Q., Hynx D., Dirnhofer S., Hess D., Ruegg C. and Hemmings B. A. (2012) Akt/PKB-mediated phosphorylation of Twist1 promotes tumor metastasis via mediating cross-talk between PI3K/Akt and TGF-beta signaling axes. Cancer Discov. 2, 248–259.

Ye P. and D'Ercole A. J. (2006) Insulin-like growth factor actions during development of neural stem cells and progenitors in the central nervous system. J. Neurosci. Res. 83, 1–6.

Zhang L., Zhou F., Drabsch Y. *et al*. (2012) USP4 is regulated by AKT phosphorylation and directly deubiquitylates TGF-beta type I receptor. Nat. Cell Biol. 14, 717–726.

Zheng W.-H., Kar S. and Quirion R. (2002) Insulin-like growth factor-1-induced phosphorylation of transcription factor FKHRL1 is mediated by phosphatidylinositol 3-kinase/Akt kinase and role of this pathway in insulin-like growth factor-1-induced survival of cultured hippocampal neurons. Mol. Pharmacol. 62, 225–233.

SUPPLEMENTAL INFORMATION FOR CHAPTER 5

Abbreviations

4E-BP	4E binding protein
AKT/PKB	Protein kinase B
BMP	Bone morphogenic protein
CNS	Central nervous system
DIV	Day-*in-vitro*
DNAse	Deoxyribonuclease
E13.5	Embryonic day 13.5
ECL	Enhanced chemiluminescence substrate
FDR	False discovery rate
FGF	Fibroblast growth factor
HBSS	Hanks balanced salt solution
IGF1	Insulin like growth factor 1
IGFBP	IGF binding protein
IGFR	IGF receptor
IIS	Insulin/IGF-signalling
IR	Insulin receptor
IRS	Insulin-like receptor substrate
mTORC	Mammalian / mechanistic target of Rapamycin complex
NFL	Negative feedback loop
NMRI	Naval medical research institute
p70-S6K	p70 ribosomal protein S6 kinase
PBS	Phosphate buffered saline
PDK	Phosphoinositide-dependent protein kinase
PI3K	Phosphoinositide 3-kinase
PPP	Picropodophyllin
PRAS	AKT1 substrate1 (Proline-rich)
PSN	Pen-Strep-Neomycin
RIPA	Radio immunoprecipitation assay buffer
RTCA	Real-time cell analysis
SGK	Serum and glucocorticoid regulated kinase
SHH	Sonic hedgehog
TBST	Tris buffered saline Tween-20
TGFβ	Transforming growth factor beta
TSC	Tuberous sclerosis complex
Wnt	Wingless (integration1)
WT	Wildtype

METHODS

Primary culture of cortical cells - Cortical cells from murine forebrain were dissected and cultured as described previously (3). NMRI wildtype (WT) mice were mated, and pregnant dams were sacrificed via cervical dislocation. Embryonic day 0.5 (E0.5) was assigned to the day of plug appearance, and cortices from E13.5 and E16.5 day old embryos were dissected in HBSS (PAA, Cölbe, Germany). Meninges were removed, and single cell suspensions were obtained by incubating chopped tissue pieces in 0.5% Trypsin-EDTA (PAA) with DNaseI (Roche, Basel, Switzerland) at 37 °C for 10 min, with subsequent trituration. Cells were counted using a hemocytometer chamber, and $1.5x10^6$ cells were seeded into one well of a double-coated 6-well plate (first Poly-L-Ornithine [0.1 mg/mL] followed by Laminin [1 µg/mL], both Sigma, Taukirchen, Germany), and cultured in Neurobasal medium supplemented with B27 (both Life Technologies, Paisley, UK), Apo-transferrin (5 µg/mL), Glutathione (1 µg/mL), Superoxide dismutase (0.8 µg/mL, all from Sigma) and PSN antibiotic mixture (1%, Life Technologies). Cells were cultured at 37 °C in a 5% CO2 incubator for 4 days *in vitro* (DIV) without changing the medium. Subsequently, cells were treated with the desired growth factor (TGFβ/IGF1) and/or inhibitor (SB431542, MK-2206, A66, TGX-221, Rapamycin, Torin 1) for the durations indicated in **Fig. 1A** for Real-time cell analysis (RTCA), immunoblots and ICCs, at the concentrations mentioned for the respective experimental procedures.

Immunocytochemistry (ICC) - Cortical cells were seeded at a density of $1x10^5$ cells onto poly-LOrnithine/Laminin pre-coated 12 mm glass coverslips, or $1.2x10^5$ cells per well of a chamber slide (BD Biosciences, Heidelberg, Germany). For TGFβ treatments, endogenous TGFβ signalling was blocked by SB431542 treatment of cultures at DIV2 (10 µM, Biozol, Eching, Germany). On DIV3, cultured cells were treated with 5 ng/mL TGFβ1 (Peprotech). Treatments with IGF1 (10nM) (Peprotech), Picropodophyllin (PPP) (500 nM), Rapamycin (100 nM) (both Calbiochem, Darmstadt, Germany), MK-2206 (1 µM), A66 (10 µM), TGX-221 (2 µM) (all Selleckchem, Munich, Germany), Torin 1 (250 nM) (Tocris), or DMSO (1:1000) (Sigma) as control,were performed on DIV4 and again on DIV6 before cells were fixed on DIV8 (**Fig. 1A**). 4% Paraformaldehyde (PFA) was used as fixative. For membrane permeabilization acetone treatment for 10 min at -20°C was performed. Unspecific antibody binding was blocked using 10% normal donkey or horse serum containing 0.1% Triton X-100 in PBS for 60 min. Coverslips were incubated overnight at 4°C with HuC/D (1:100, A- 21271, Invitrogen, Darmstadt, Germany) or activated Caspase3 (1:500, #9669, Cell Sig-

nalling Technology). Both primary antibodies were diluted in blocking solution. Donkey anti-mouse (Alexa 568) secondary antibody (Jackson ImmunoResearch, West Grove, PA) (against HuC/D) and antirabbit secondary antibody (Alexa 488) (against aCASP3) was added the next day at a dilution of 1:500 in PBS, incubated for 1 h at room temperature and cells were subsequently counterstained with DAPI (1:1000, Sigma). Cell proliferation through BrdU was assessed using a BrdU-labelling Kit (#11299964001, Roche, Basel, Switzerland). BrdU pulse was applied for 60 min before fixing on DIV 6 (**Fig. 1A**). Staining was performed according to the manufacturer's instructions. Coverslips and chamber slides were mounted with Fluoromount-G (Southern Biotechnology, Birmingham, AL, USA) or DAKO Fluorescent Mounting Medium (DAKO, Hamburg, Germany) and visualized using an Axio Imager Z1 microscope (Carl Zeiss, Göttingen, Germany). For one experimental set, at least 8 random fields were used for quantification. Independent experiments were performed using cells from different animals per experiment, and collected data are represented as the mean ± standard error of means (SEM). Quantification was performed via an in house-designed macro with ImageJ. Quantification of BrdU, HuC/D and aCASP3 positive cells is expressed as percentage of DAPI-positive nuclei. Statistical assessment to verify differences between treatments in terms of p-values was performed using Students' t-test.

Microarray analyses - Gene expression profiles of primary cortical cells obtained from E13.5 and E16.5 NMRI mice were quantified using Agilent's Mouse Genome Microarray (G4846A). Cells derived from E13.5 and E16.5 forebrains were treated with SB431542 (10 μM) on DIV2 to suppress endogenous TGFβ-signalling, and half of them with TGFβ on DIV3. Cells from both conditions were harvested on DIV4. Total RNA from these cells was extracted using Trizol reagent (Invitrogen), and Cy3 and Cy5 intensities were detected by two-colour scanning, performed at a resolution of 5 μm using an Agilent DNA microarray scanner (G250B). All steps of the analysis were performed with normalized data on the log2-scale using MATLAB and the R statistical programming environment (R.DevelopmentCoreTeam 2012). For quality control, hierarchical clustering was performed to validate the groups. To check whether the data satisfied the mathematical assumptions underlying the statistical tests (such as normal distribution and independence of the measurement noise), the empirical distributions of the p-values were evaluated. Linear statistical models as implemented in the limma package (Smyth 2005) were applied to estimate fold changes and for assessing significance. To stabilize the analysis, the moderated t-statistic was used. The false discovery rate (FDR) was estimated using the so-called Benjamini-Hochberg approach (Benjamini & Hochberg 1995) to account for multiple testing.

Real-time Cell Analyses - Real-time cell analyses (RTCA) were performed with an RTCA-system (xCELLigence, Roche, Basel, Switzerland). Poly-L-Ornithine/ Laminin-coated 16-well E-plates (Roche), filled with 100 µL of supplemented Neurobasal medium, were used for background measurements. Subsequently, 60,000 primary cortical cells obtained from E13.5 or E16.5 embryos were seeded into 100 µL medium per well. After allowing cells to settle into the wells (30 min at room temperature), RTCA was started at 37 °C in a 5% CO2 incubator. Cell growth was recorded for 72 h at 15 min intervals. After 24 h (E13.5) or 8 h (E16.5) inhibitors were added to the medium **(Fig. 1A)** using the following concentrations: PPP (500 nM), Rapamycin (100 nM), MK-2206 (1 µM), Torin 1 (250 nM), or 1:1000 DMSO (1:1000) as control. For data analyses, each curve was normalised to the point of treatment (indicated in figures 2D, 3A, 3B, 3H by the dashed vertical line). One representative out of at least three independent experiments is shown.

Immunoblotting - To assess for signalling kinetics, cells were treated with IGF1, IGF2, PPP, MK- 2206, A66, TGX-221, SB431542 and TGFβ as short pulses of 10-60 min prior to harvesting (**Fig. 1A**), as indicated in individual immunoblots. The treatment durations for each experiment are as shown in the individual immunoblot images. The following concentrations were used: 10 µM SB431542, 5 ng/mL TGFβ1, 10 nM IGF1 or IGF2, 500 nM PPP, 100 nM Rapamycin, 1 µM MK-2206, 10 µM A66, 2 µM TGX-221, 250 nM Torin 1, or 1:1000 DMSO as control, respectively. Cortical cell pellets were resuspended and lysed in RIPA buffer (1% each of NP-40, PBS, SDS, and 0.5% Sodium deoxycholate in deionized water), supplemented with protease- (Complete, Roche, Basel, Switzerland) and phosphatase-inhibitors (Phosphatase Inhibitor Cocktail 3, Sigma). After trituration, samples were subjected to sonication in a Bioruptor (Diagenode, Liege, Belgium) for 10 cycles with 10 s intervals between each cycle, spun at 13,362 x g for 10 min, and the supernatant was transferred to fresh 1.5 mL Eppendorf tubes. Protein concentration was measured spectrophotometrically by the Bradford reagent assay (Bio-Rad, Munich, Germany) and absorbance measured at 595 nm, using reducing BSA concentrations as standards. Samples were adjusted in 5x Lämmli buffer, boiled for 5 min at 95 °C, and 20-30 µg protein was loaded per well of an 8-15% SDS poly-acrylamide gel and run at 100 V for 1.5 h. Post-electrophoresis, samples were transferred onto Polyvinylidene difluoride (PVDF) membranes (Milipore, Schwalbach, Germany) for 1.5 h. Subsequently, membranes were blocked for 20 minutes in 5% BSA (PAA) solution in 1x TBST and incubated overnight with the primary antibody. After washing and incubating with secondary antibody for 1 h at room temperature proteins were visualised

with ECL and Femto chemiluminescent substrates (both, Thermo Scientific, Bonn, Germany) using an LAS-ImageQuant detection system (Fujifilm/GE Healthcare, Freiburg, Germany). All primary antibodies were used at a concentration of 1:1000, diluted in 5% BSA in TBST, containing 0.01% Sodium Azide (Roth, Germany). Peroxidase-conjugated anti-mouse (#31430), antirat (#31470) and anti-rabbit (#31460) secondary antibodies (both Thermo Scientific) and anti-goat (sc-2020, Santa Cruz Biotechnology) were used at a concentration of 1:10,000. Following primary antibodies were used: AKT-pan # 4691, AKT-pT308 #2965, AKT-pS473 #4060, IGF1Rβ #111A9, #3018, IGF1Rβ-pY1135 #3918, IGF1Rβ-pY980 #4568, IRS1 #2382, IRS1-pS636/639 #2388, PRAS40 #2691, p70-S6K #9202, p70-S6K-pT389 # 9206, SMAD2 #3122, SMAD2-pS465/467 #3108, SMAD3 #9523, SMAD3-pS423/425 #9520 (Cell Signalling Technologies, Frankfurt, Germany), IGF1 #AF791, IGFBP3 #MAB775 (RnD Systems, Wiesbaden-Nordenstadt, Germany), GAPDH #8245 and HSC70 #19136 (Abcam, Cambridge, UK), PRAS40-pS183 – IBL #JP28035, TGFβ1 #ARP37894 (Aviva Systems Biology, San Diego, CA, USA), TGFβ2 #sc-90, TGFβ3 #sc-82 (SantaCruz Biotechnology Inc., Heidelberg, Germany), and α-Tubulin #2871-1 (Epitomics, Burlingame, CA, USA).

Immunoblot quantification - Densitometric measurements for all immunoblots were performed using ImageJ. Band intensities were analyzed relative to the experimental control (GAPDH) and denoted as "Normalised Intensity". For p70-S6K-pT389 the upper band at 70 kDa, for PRAS40-pS183 the upper band at 40 kDa and for AKT-pT308 both bands at 60 kDa were measured. Depending on the context, the control experiment is given by the DMSO control or by the respective measurements at day 13.5 and normalized to 1. The error bars depicted in the figures have been calculated based on the law of error propagation, i.e. if a function $f(x,y)$ of two variables x and y with measurement errors $\sigma(x)$ and $\sigma(y)$ is of interest, the error of f is given by

$$\sigma(f) = \sqrt{\left(\frac{\partial f}{\partial x}\right)^2 \sigma(x)^2 + \left(\frac{\partial f}{\partial y}\right)^2 \sigma(y)^2}\,.$$

This yields, as an example, the relationship $SEM = SD/\sqrt{n}$ between the standard deviation SD and the standard error of the mean (SEM) for averaging of n experimental replicates. For a ratio $R = \frac{x}{y}$ the law of error propagation yields

$$\sigma(R) = R\sqrt{\left(\frac{\sigma(x)}{x}\right)^2 + \left(\frac{\sigma(y)}{y}\right)^2}$$

All measurements were made from independent experiments, with experimental replicates ranging from at least three repetitions, as specified for each figure.

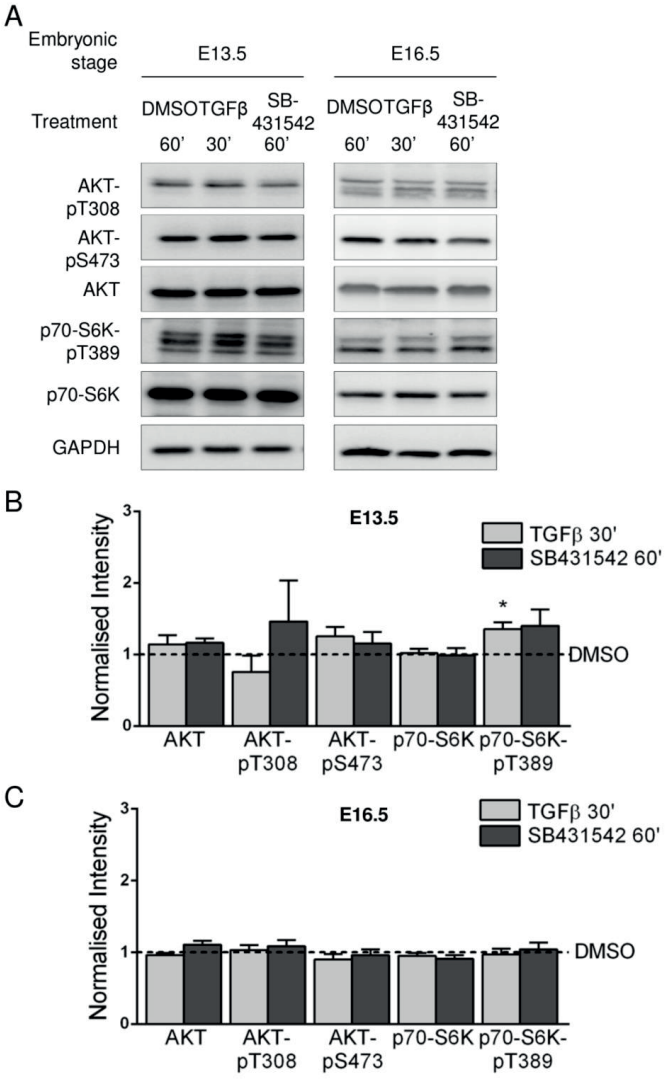

Fig. S1: TGFβ-signalling did not induce PDK1-AKT-mTOR-signalling in E13.5- and E16.5-derived cortical cells.

(A) Immunoblots of proteins from E13.5- and E16.5-derived cortical cells assessing PDK1, AKT-, mTORC1- and mTORC2-activation after treatment with DMSO (60 min), TGFβ (30 min) or SB431542 (60 min) are shown. (B) Densitometric measurements for AKT and p70-S6K total and phosphorylated forms upon the above treatments are shown. Given is the normalised intensity of signals fromTGFβ- and SB431542-treated cells. Intensities from DMSO-treated cells were chosen as control level and set to 1 as indicated by the horizontal dashed line. p-value p70-S6K-pT389 in E13.5-derived cells = (E13.5: n=3, E16.5: n=8).

Supplementary Table S1

LogFC values of developmentally regulated genes (E16.5 vs. E13

Gene Symbol	Log FC expression at E16.5
Igf2	-11.7
Igf1	-10.3
Igf2bp1	-5.1
Isl1	-4.92
Igfbprp	-4.65
Wisp1	-4.65
Igf2bp2	-3.9
Rhoj	-3.64
Grb10	-3.0
Rnd3	-2.81
Cdkn2b	-2.8
Igfbp4	-2.8
Igfbp5	-2.6
Cdk2	-2.5
Cdkn3	-2.5
Pik3r3	-2.5
Ccnb1	-2.4
CycD2	-2.4
Insl6	-2.38
Il1r1	-2.23
Il1rl2	-2.21
IRS1	-2.18
Rhod	-2.06
Vegfc	-2.06
Vegfc	-2.06
Igf2bpl1	-2.03
Map3k6	-2.01

Gene Symbol	Log FC expression at E16.5
Cdkl2	2.01
Rhou	2.0
Rragd	2.07
Rasgrf2	2.09
Myc	2.1
Mapt	2.11
Prkcb	2.0
Prkaa2	2.27
Cdkl5	2.3
Prkar1b	2.0
Ppp2r2c	2.0
Pik3r1	2.43
Rps6kl1	2.5
Pik3cd	2.7
Cdc25b	3.0
Sgk1	3.15
Prkcq	3.17
Pla2g4e	4.07
Mef2c	5.97
Hspb3	7.6